**Chimica et Natura Acta**
p-ISSN: 2355-0864 e-ISSN: 2541-2574
Homepage: http://jurnal.unpad.ac.id/jcena

# Biosynthesis, Characterization of Curcumin-Capped Zno-Cuo and Chitosan-Curcumin-Capped Zno-Cuo based Nanomaterial as Antibacterial Agent of *Escherichia coli*

Ahmad Fatoni[1]*, Afnita Fatmawati Umli[1], Reza Agung Sriwijaya[1], Hilma Hilma[1], Nurlisa Hidayati[2]

[1]Pharmacy Study Program, Bhakti Pertiwi College of Pharmaceutical Sciences, Jln. Ariodillah III No. 22 Palembang, South Sumatera.
[2]Department of Chemistry, Faculty of Mathematic and Natural Sciences, Sriwijaya University, Jln. Palembang-Prabumulih Km. 32 Indralaya Ogan Ilir, South Sumatera.
*Corresponding author: tonistifibp@gmail.com

DOI: https://doi.org/10.24198/cna.v13.n3.62946

**Abstract:** The biofabrication of the chitosan-curcumin-capped ZnO-CuO and curcumin-capped ZnO-CuO nanoparticles, as well as their ability to combat *Escherichia coli* bacteria, were the focus of this study. Fourier-Transform Infrared (FTIR) spectroscopy, X-ray diffraction (XRD), and Scanning Electron Microscopy (SEM) were used to examine the chitosan-curcumin-capped ZnO-CuO and curcumin-capped ZnO-CuO nanoparticles, respectively. Both were evaluated using the agar diffusion method as antibacterials against Escherichia coli. Results of analysis with FTIR, between 500 and 700 $cm^{-1}$, the functional group of Cu-O or Zn-O was seen at its highest point. The functional group of Cu-O and Zn-O in curcumin-capped ZnO-CuO was detected at wavenumber of 621 $cm^{-1}$ and 507 $cm^{-1}$, respectively. In chitosan-curcumin-capped ZnO-CuO, the wave numbers of the Cu-O and Zn-O groups were observed at 619 and 653 $cm^{-1}$ respectively. According to XRD analysis results, the chitosan-curcumin-capped ZnO-CuO and curcumin-capped ZnO-CuO nanoparticles' crystalline shapes are demonstrated by their respective crystallite sizes of 12.58 and 1.88 nm. Based on the results of analysis with SEM, curcumin-capped ZnO-CuO and chitosan-curcumin-capped ZnO-CuO nanoparticles have a dense surface structure. The average diameter of inhibition zone (clear zone) produced by chit-cur-ZnO-CuO nanoparticles is 14.61 mm, while the clear zone produced by cur-ZnO-CuO nanoparticles is 9.52 mm. Chit-cur-ZnO-CuO has superior antibacterial qualities to cur-ZnO-CuO nanoparticles.

**Keywords:** chitosan, curcumin, ZnO-CuO, *Escherichia coli*

***Abstrak:*** *Biofabrikasi kitosan-kurkumin yang dilapisi ZnO-CuO dan kurkumin yang dilapisi ZnO-CuO nanopartikel, serta sifat antibakterinya terhadap Escherichia coli, menjadi subjek penelitian ini. Spektroskopi FTIR, difraksi sinar-X (XRD), dan mikroskop elektron pemindaian (SEM) digunakan untuk analisa kitosan-kurkumin yang dilapisi ZnO-CuO dan kurkumin yang dilapisi ZnO-CuO nanopartikel. Keduanya dievaluasi menggunakan metode difusi agar sebagai antibakteri terhadap Escherichia coli. Hasil analisis dengan FTIR, bilangan gelombang antara 500 dan 700 $cm^{-1}$, merupakan gugus fungsi Cu-O atau Zn-O. Gugus fungsi Cu-O dan Zn-O pada kurkumin yang dilapisi ZnO-CuO nanopartikel terdeteksi masing-masing pada bilangan gelombang 621 $cm^{-1}$ dan 507 $cm^{-1}$. Pada kitosan-kurkumin yang dilapisi ZnO-CuO nanopartikel, bilangan gelombang gugus fungsi Cu-O dan Zn-O terdeteksi masing-masing pada bilangan gelombang 619 dan 653 $cm^{-1}$. Hasil analisis dengan XRD menunjukkan bentuk kristal kitosan-kurkumin yang dilapisi ZnO-CuO nanopartikel dan kurkumin yang dilapisi ZnO-CuO nanopartikel, ditunjukkan oleh ukuran kristalinitas masing-masing sebesar 12,58 dan 1,88 nm. Berdasarkan hasil analisis dengan SEM, kurkumin yang dilapisi ZnO-CuO nanopartikel dan kitosan-kurkumin yang dilapisi ZnO-CuO nanopartikel memiliki struktur permukaan yang padat. Diameter rata-rata zona hambat (zona bening) yang dihasilkan oleh kitosan-kurkumin yang dilapisi ZnO-CuO nanopartikel adalah 14,61 mm, sedangkan zona bening yang dihasilkan oleh kurkumin yang dilapisi ZnO-CuO nanopartikel adalah 9,52 mm. Kitosan-kurkumin yang dilapisi ZnO-CuO nanopartikel memiliki kualitas antibakteri yang lebih unggul dibandingkan kurkumin yang dilapisi ZnO-CuO nanopartikel.*

***Kata kunci:*** *kitosan, kurkumin, ZnO-CuO, Escherichia coli*

## INTRODUCTION

The study of materials with a nanoscale range of 1–100 nm is the main focus of the diverse field of nanotechnology. Food, cosmetics, medicine, healthcare, electronics, chemicals, and agriculture have all benefited greatly from nanotechnology (Malik *et al*. 2023). Nanoscale, nanoparticle, nanomaterial, nanocomposite, and nanostructured materials are the core ideas in the field of nanotechnology (Szczyglewska *et al*. 2023). The scientific community accepts goods and technologies that are safer, cleaner, and more reasonably priced than those of the past as science and technology advance. Thus, nanotechnology offers a solution to this issue. In contrast to previous heavy equipment and mass bulking, this approach is more transparent, cleaner, and less expensive (Malik *et al*. 2023)

A potential field of nanotechnology that appeals to material scientists, chemists, and biologists is the synthesis of metal nanoparticles (MNPs) from low-cost, highly effective biological sources. The absence of toxic chemical compounds used as stabilizing or reducing agents, which results in biocompatibility, the lack of toxic yield produced by this process, its low energy consumption at a reasonable cost, and its high scalability are some of the notable characteristics of the green (biosynthesis) technique (Bordiwala 2023). Because of their enhanced physicochemical, optical, mechanical, and electrical properties, bio nanoparticles made possible by the green approach are more comparable to metal oxide (MeO) nanoparticles in terms of their applicability (Aigbe & Osibote 2024).

The biosynthesis of bimetallic nanoparticles is currently in vogue. The right combination of two distinct metals with improved reaction capabilities and features essentially makes up bimetallic nanoparticles. Because of this, this kind of material has garnered a lot of interest from both a scientific and technological standpoint. Due to biosynthesis employing plant parts like leaves, double (bimetallic) nanoparticles have gained more attention. According to some earlier research, ZnO-CuO nanoparticles were biosynthesised using plant extracts from plants like *Tragia involucrata* L. (Jeevarathinam & Asharani 2024), *Sambucus nigra* L. (Cao *et al*. 2021), *Psidium guajava* (Fatoni *et al*. 2023a; Fatoni *et al*. 2023b), *Artemisia vulgaris* (Nepal *et al*. 2024), *Berberis vulgaris* (Yousefinia *et al.* 2023), *Dovyalis caffra* (Adeyemi *et al*. 2022), *Verbascum sinaiticum* Benth (Bekru *et al*. 2022) and *Artemisia abyssinica* (Orshiso *et al*. 2023).

Dadi *et al*. (2019) reported when bacteria were in their exponential growth phase, the CuO and ZnO nanoparticles demonstrated equivalent efficacy. There is a synergistic effect between ZnO and CuO nanoparticles as antibacterial for *E. coli* (Abbas *et al*. 2024). The combination of ZnO and CuO nanoparticles has significant antibacterial properties (Govindasamy *et al.* 2021; Widiarti *et al.* 2017; Dhage *et al.* 2024).

One important chitin derivative that has caught the interest of researchers is chitosan. Because it is renewable, non-toxic, soluble in aqueous solutions, biocompatible, and environmentally benign, it has gained popularity in recent years (Alzahrani 2018). For ZnO-CuO nanoparticles, chitosan can serve as a matrix or supporting material. The resulting chitosan-ZnO-CuO nanoparticles can be employed as an antioxidant, antibacterial, and for dye photodegradation (Alzahrani 2018; Fatoni *et al.* 2023a; Fatoni *et al.* 2023b; Kalia *et al.* 2021; Gamboa-Solana *et al.* 2021. The aforementioned justifications for employing chitosan as a supporting matrix for bimetallic oxide nanoparticles include enhancing the mechanical and physical qualities of chitosan (Ali *et al.* 2024) and the biological and adaptive qualities of chitosan-(bi) metallic oxide nanoparticles (Al-Rajhi *et al.* 2024).

The rhizomes of *curcuma longa* L. (turmeric) are used to extract the nutraceutical chemical curcumin (1,7-bis(4-hydroxy-3-methoxyphenyl)-1,6-heptadiene-3,5-dione). The herb curcuma longa's rhizome yields curcumin, a hydrophobic polyphenolic molecule (Madian *et al*. 2023). Chitosan and other biopolymers can interact with curcumin to enhance the materials' bioavailability and therapeutic effectiveness (Karthikeyan *et al.* 2020). The qualities of chitosan film are improved by adding curcuma ethanol extract to chitosan in chitosan film products (Rachtanapun *et al.* 2021; Madian *et al.* 2023). According to Liu *et al.* (2016), Etemadi *et al.* (2021), Jahromi *et al.* (2014), and Azkia *et al.* (2020), chitosan and curcumin together have antibacterial and antioxidant properties. Carboxy methyl chitosan modified by curcumin as antibacterial (Kabiriyel *et al.* 2023) and chitosan nanocomposite prepared by curcuma extract for cancer treatment (Zulkifli *et al*. 2022; Deepika *et al.* 2022).

Curcumin-chitosan can be used as a biocompatible alternative to metallic nanoparticles (Khezri *et al.* 2018), and curcumin-chitosan combined with metallic nanoparticles can have antibacterial properties (Karthikeyan *et al.* 2020). Combining two metal oxides results in a mixture with numerous significant properties, including a high surface area and remarkable heat stability. They can perform tasks like antimicrobial activity more successfully because they have more active patches on their surface, which enhances their reaction time (Takele *et al.* 2023) and finally, coating the surface of nanomaterial curcumin-ZnO-CuO with chitosan will increase the antibacterial properties of ZnO-CuO nanoparticles.

In this study, chitosan-curcumin capped ZnO-CuO nanoparticles (chit-cur-ZnO-CuO nanoparticles) were prepared and utilized as an antibacterial against *E. coli*. This is based on chitosan as a biocompatible

polymer and has antibacterial properties (Sanmugam *et al.* 2024), curcumin as a principal reducing agent and stabilizing compounds in the production of metallic nanoparticles (Patra & El Kurdi 2021), metal oxides with inherent antibacterial and the ability to generate reactive oxygen species (ROS) (Ren *et al.* 2020) and the combination of these materials leads to a synergistic antimicrobial effect than individual components. These nanomaterials were characterized using scanning electron microscopy (SEM), X-ray diffraction (XRD), and Fourier-transform infrared spectroscopy (FTIR). Additionally, the agar diffusion method was used to assess these nanoparticles' antibacterial efficacy.

## MATERIALS AND METHOD

### Materials and Equipment

These include nutritional agar, sodium hydroxide, zinc acetate pentahydrate, copper sulphate pentahydrate, and glacial acetic acid (Merck) except chitosan (DD 87%). Aquadest is one of the *Escherichia coli* bacteria that we utilize in our lab. Palembang's *curcuma longa*. X-Ray Diffraction (Shimadzu XRD 6000), Scanning Electron Microscopy (Axia ChemiSEM, Thermo Fisher Scientific), Ultra Violet-Visible (UV-Vis Genesys 150 Thermo Scientific) and FTIR spectrophotometer (Shimadzu Prestige-21). Hot Plate (HS 7 IKA C Mag), Oven (model DHG - 9053 A) and Analytical Balance (VIBRA Shinko Denshi). The equipment used is standard laboratory glassware (pyrex).

### Ethanolic Extract as Medium in Biosynthesis

In a nutshell, 250 mL of solvent (ethanol 96%, v/v) is added to a maceration bottle containing 25 grams of freshly grated turmeric (*Curcuma longa*) and left for 48 hours. Macerate (I) was produced by filtering the solution after 48 hours to remove the solid material from the extract solution. After 48 hours of macerating the solid material once more with 96% ethanol (v/v, 250 mL), the solution was decanted to produce macerate (II). For usage in the biosynthetic process (ethanolic extract of *curcuma longa*), macerates I and II are mixed.

### Curcumin-capped zinc oxide-copper oxide nanoparticles biofabrication

With minor adjustments, this process is based on earlier studies (Arab *et al.* 2021; Karthikeyan *et al.* 2020). In a 500 mL beaker glass, 200 mL of *curcuma longa* ethanolic extract is combined with 0.1 M, 100 mL solutions of zinc acetate dihydrate and copper sulphate pentahydrate. After that, the mixture was constantly mixed (60 minutes, 25°C). The mixture's pH was raised to 9 by adding 0.8 M NaOH solution. After that, the whole mixture was heated to 80°C while being constantly stirred. At room temperature, the residual mixture was allowed to precipitate for a single night. In a vacuum oven set at 80°C, the precipitate (curcumin-capped ZnO-CuO nanoparticles) was completely cleaned using distilled water and a 96% v/v ethanol solution. The precipitate was then dried until it was completely dry.

### Chitosan-curcumin-capped zinc oxide-copper oxide nanoparticles biofabrication

With minor adjustments, the biosynthesis process was taken from Arab *et al.* (2021) and Karthikeyan *et al.* (2020). A 500 mL beaker containing solutions of copper sulphate pentahydrate (0.1 M, 100 mL) and zinc acetate dihydrate (0.1 M, 100 mL) was filled with a 2% w/v chitosan solution (2 g of chitosan, 100 ml of acetic acid 3% v/v). For half an hour, the mixture was constantly swirled at room temperature. After adding 200 mL of *curcuma longa* ethanol extract, the mixture was constantly agitated for an hour at room temperature. NaOH solution (0.8 M) was added after an hour until the pH reached 9. At 80°C, the mixture was heated while being constantly stirred. After that, the mixture is precipitated for the entire night until a solid that separates from the liquid is formed. Following separation, the solid is washed with 96% v/v ethanol and distilled water. The solids (chitosan-curcumin-capped ZnO-CuO nanoparticles) were dried in an oven set to 80°C.

### Antibacterial study

Curcumin-capped ZnO-CuO and chitosan-curcumin-capped ZnO-CuO nanoparticles were tested for their antibacterial properties utilizing the diffusion method on the *E. coli* bacterial strain. *Escherichia coli* bacteria were used as the microbial inoculum. Briefly, to create the inoculum suspension, sterile 0.9% NaCl solution was added to a fresh culture, shaken, and the optical density at 580 nm was measured and adjusted until the inoculum's transmittance was 25% (Isnaeni *et al*. 2020) and the nutrient agar that had solidified in the plates was swabbed onto 10 mL of nutrient agar that had been created in petri plates (Fatoni *et al.* 2023b). In order to assess the antibacterial activity, 1.5 %, and 2 % of curcumin-capped ZnO-CuO nanoparticles and chitosan-curcumin-capped ZnO-CuO nanoparticles were disseminated in 10 mL of dimethyl sulfoxide (DMSO). After 24 hours of overnight incubation at 37°C, the zones of inhibition levels were determined. The positive and negative controls in this case were DMSO and regular chloramphenicol, respectively. Every test was conducted in triplicate.

### Characterization

FTIR, XRD, and SEM were used to characterize the curcumin-capped ZnO-CuO and chitosan-curcumin-capped ZnO-CuO nanoparticles, respectively. With a wave number range of 400 to 4000 $cm^{-1}$, functional groups curcumin-capped ZnO-CuO and chitosan-curcumin-capped ZnO-CuO nanoparticles were examined using FTIR. In order to determine their crystallinity size, both were subjected to physical structural analysis using XRD. A Cu Kα

X-ray tube with a scan speed and duration time of 10,000 degrees per minute, running at 1.5406 Å, 30 kV, and 10 mA, and a 2Θ range of 0° to 90°, is the operating condition for X-ray diffraction. Both were examined for surface morphology using SEM at 10.00 Kv at x 3500 magnifications (scale bars = 5 $\mu$m).

## RESULT AND DISSCUSION

### The process by which chitosan-curcumin-capped ZnO-CuO and curcumin-capped ZnO-CuO nanoparticles are formed

The image of the biosynthesis process is as shown in Figure 1. The current study uses the phenolic groups found in turmeric extract as a reduction technique to create curcumin-capped ZnO-CuO nanoparticles (Yazdani *et al.* 2023). Compared to naked curcumin, curcumin-capped ZnO-CuO nanoparticles have a comparatively greater surface area for solvent interaction. This characteristic increases their solubility in water, which enhances the bound's bioavailability (Venkatas *et al*. 2022).

The ability of the reaction pH to alter the electrical charges of biomolecules may have a significant impact on their capacity to cap and stabilize, which may in turn have an impact on the development of nanoparticles (Khalil *et al.* 2014; Mohammadi & Ghasemi 2018). Metal oxide nanoparticles have high solubility in low pH regions and partial disaggregation at high pH, with a pH range of 4 to 10 being advised (Mohammadi & Ghasemi 2018).

The reaction of precursors (zinc acetate dihydrate and copper sulphate pentahydrate) with polyphenols (R-OH in curcumin) to produce an intermediate chemical (zinc or copper hydroxide) is one potential mechanism for curcumin-capped ZnO-CuO nanoparticles biosynthesis. The heat generated during the drying step subsequently converts this chemical into either copper oxide or zinc oxide, as indicated by the subsequent reactions (Alallam *et al.* 2023):

A carbon-nitrogen double bond (Schiff base), which is the nucleophilic creation of the nitrogen atom of the amino group ($-NH_2$) that produces chitosan-curcumin-capped ZnO-CuO nanoparticles, can be formed when chitosan binds to the carbonyl carbon (C=O) of the chemical structure curcumin (Karthikeyan *et al*. 2020).

### FTIR result

Figure 2 provides an explanation of the FT-IR spectra of curcumin, curcumin-capped ZnO-CuO, and chitosan-curcumin-capped ZnO-CuO nanoparticles.

$$Zn(CH_3CO_2)_{2\,(aq)} + 2R\text{–}OH_{(aq)} \rightarrow Zn(OH)_{2\,(s)} + 2R\text{–}CH_{(3)}CO_{2\,(aq)} \quad ...(1)$$

$$Zn(OH)_{2\,(s)} + \text{heat} \rightarrow ZnO_{(s)} + H_2O_{(v)} \quad ...(2)$$

$$CuSO_{4\,(aq)} + 2R\text{–}OH_{(aq)} \rightarrow Cu(OH)_{(2)\,(s)} + 2R\text{–}SO_{4\,(aq)} \quad ...(3)$$

$$Cu(OH)_{2\,(s)} + \text{heat} \rightarrow CuO_{(s)} + H_2O_{(v)} \quad ...(4)$$

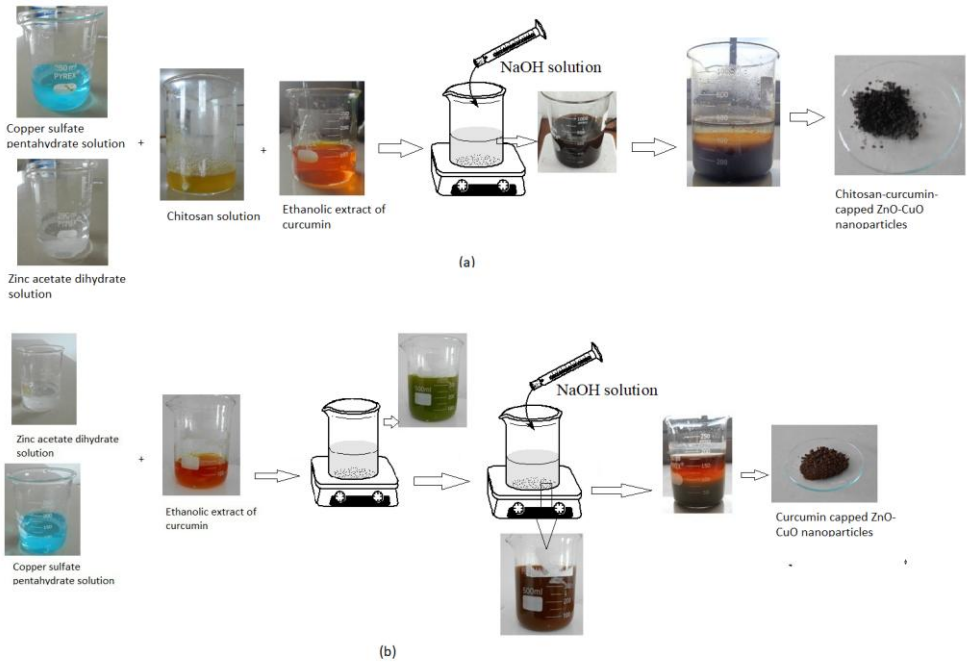


**Figure 1**. Representative image of biosynthesis chitosan-curcumin-capped ZnO-CuO (a) and curcumin-capped ZnO-CuO nanoparticles (b)

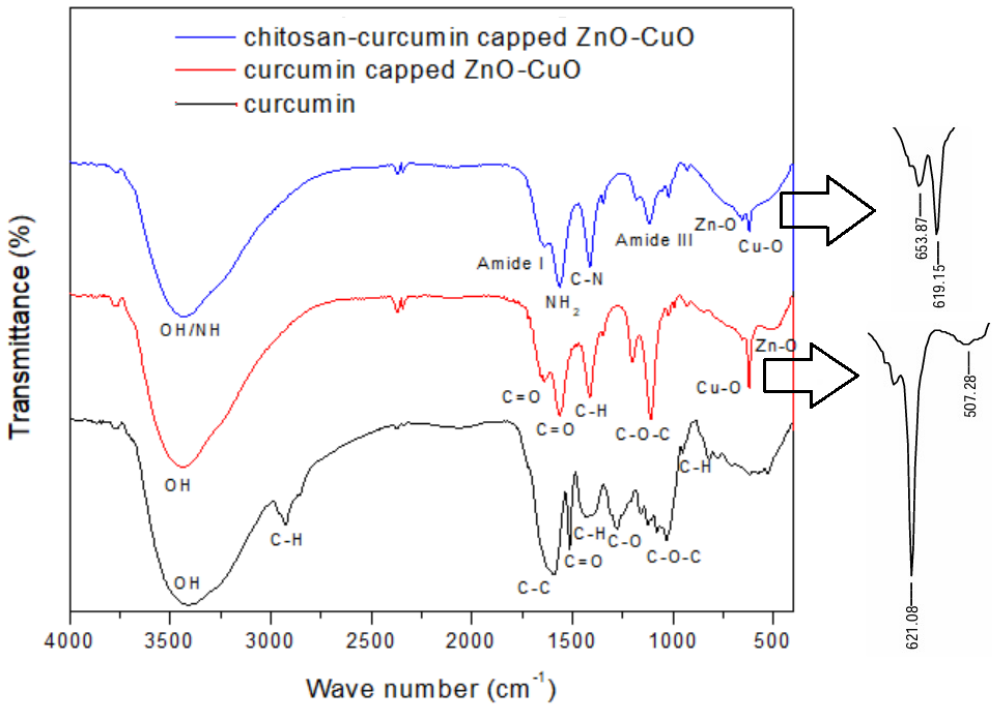


**Figure 2**. FTIR spectra of curcumin, curcumin-capped ZnO-CuO and chitosan-curcumin-capped ZnO-CuO nanoparticles

In curcumin, the FTIR spectrum showed characteristic stretching bands and peaks matching with the FTIR spectra reported in the literature. The OH stretch was observed at 3415 $cm^{-1}$ (3427 $cm^{-1}$ by Sathiyabama *et al*. 2020). The C-H stretch as $CH_2$ and $CH_3$ asymmetric stretching was observed at 2924 $cm^{-1}$ (2916 $cm^{-1}$ by de Rocha *et al.* 2020). At 1593 $cm^{-1}$, the distinctive aromatic (C=C) band was detected (602 $cm^{-1}$ by Sathiyabama *et al*. 2020). A band at 1512 $cm^{-1}$ is assigned to (C=O) (1508 $cm^{-1}$ by de Rocha *et al.* 2020; 1509 $cm^{-1}$ by Saif *et al.* 2024; 1516 $cm^{-1}$ by Qasem *et al*. 2020). $CH_2$ band was observed at 1429 $cm^{-1}$ (1422 $cm^{-1}$ by de Rocha *et al.* 2020). The measurement of the phenolic stretch (C-O) was 1276 $cm^{-1}$ (1278 $cm^{-1}$ by Qasem *et al.* 2020; 1284 $cm^{-1}$ by de Rocha *et al.* 2020; 1280 $cm^{-1}$ by Saif *et al.* 2024; 1281 $cm^{-1}$ by Sathiyabama *et al.* 2020). The 1031 $cm^{-1}$ peaks are attributed to C-O-C (1025 $cm^{-1}$ by Saif *et al.* 2024) and at 994 $cm^{-1}$, the benzoate trans-CH vibration peak was discovered (962 $cm^{-1}$ by de Rocha *et al.* 2020 & Saif *et al.* 2024).

Using Fourier-transform infrared (FT-IR), the transmittance of the curcumin-capped ZnO-CuO nanoparticles as a function of wavenumber has been used to examine their surface characteristics. The FTIR spectra of the curcumin-capped ZnO-CuO nanoparticles showed the stretching bands at wavenumbers of 3444 $cm^{-1}$ due to the presence of –OH intermolecular (El-Kattan *et al.* 2022). According to Saif *et al.* (2024), there are distinctive absorption bands at 1564 $cm^{-1}$ because of C=O stretching, at 1411 $cm^{-1}$ because of C−H bending, and at 1090 $cm^{-1}$ because of C−O−C stretching vibration. However, one peak was obtained in this region at 1639 $cm^{-1}$ for the curcumin-capped ZnO-CuO nanoparticles, where the 1639 $cm^{-1}$ peak could be due to $\nu$(C=O) of curcumin (Moussawi & Patra 2016). In curcumin-capped ZnO-CuO nanoparticles, the main characteristic peak of Zn-O is located in the range of 500–700 $cm^{-1}$, indicating the stretching of the Zn–O bond (Mosallanezhad *et al.* 2022). Another reference, the peak in the range 500–700 $cm^{-1}$, should be a stretching of Cu-O (Qasem *et al.* 2020). The FTIR spectrum showed the expected Cu−O and Zn−O stretching vibrations at 621 $cm^{-1}$ and 507 $cm^{-1}$, respectively (Qasem *et al*. 2020; Mosallanezhad *et al.* 2022; Madeo *et al.* 2023).

The band's position in this FTIR spectrum changed from 3415 $cm^{-1}$ to 3444 $cm^{-1}$, suggesting that these phenolic hydroxyls interacted with ZnO-CuO nanoparticles (Moussawi & Patra 2016). The absence of bands at 3500 $cm^{-1}$ and 1600 $cm^{-1}$, which are often ascribed to the hydroxyl functional group's O–H stretching vibration peak and the surface H–OH bending vibration, indicates that there was no hydroxyl group adsorption on the ZnO–CuO nanoparticle surface. Curcumin chelates with ZnO-CuO nanoparticles through the enol form, according to current FTIR study.

Chitosan-curcumin-capped ZnO-CuO nanoparticles'FTIR spectrum shows the main characteristic peaks of curcumin, chitosan and ZnO-CuO nanoparticles. For the functional group of curcumin, Karthikeyan *et al.* (2020) reported in the region between 1750 and 750 $cm^{-1}$ was overlapping of the functional group of chitosan and curcumin. A peak at 1639 $cm^{-1}$ for amide I group of chitosan (Ramalingam *et al.* 2015). Amide II from chitosan

was observed at 1564 $cm^{-1}$ (Ramalingam *et al.* 2015) and C=C for curcumin (Sathiyabama *et al.* 2020). Amide III was detected at 1411 $cm^{-1}$ for C–N stretching vibrations (El-Naggar *et al.* 2022). A peak at 1180 $cm^{-1}$ for asymmetric stretching of the C-O-C bridge and 1116-1020 $cm^{-1}$ for C-O stretching (Enumo *et al.* 2020). Zn-O and Cu-O group were noted at 653 and 619 respectively (Soumya *et al.* 2017; Qasem *et al*. 2020).

In addition, the peak relating to the –OH/–$NH_2$ stretching vibration in chitosan (at 3450 $cm^{-1}$) is shifted to the lower wavenumber (3442 $cm^{-1}$) in the FTIR spectra of chitosan-curcumin-capped ZnO-CuO nanoparticles, suggesting the strong intermolecular hydrogen bonding interaction between chitosan and ZnO-CuO nanoparticles (Nguyen *et al*. 2020) and these interactions are due to the electrostatic interaction between chitosan and ZnO-CuO nanoparticles in the chitosan-curcumin-ZnO-CuO nanoparticles surface matrix (Karthikeyan *et al.* 2020). The C=O functional group of curcumin (1512 $cm^{-1}$) does not appear in this FTIR spectrum of curcumin-capped ZnO-CuO nanoparticles but the wave number of 1658 $cm^{-1}$ in chitosan becomes lower in this FTIR spectrum (1639 $cm^{-1}$). This change is possible due to the formation of a schiff base functional group between the C=O functional group of curcumin and the $NH_2$ of chitosan (Karthikeyan *et al.* 2020; Saranya *et al.* 2018; Kocak *et al.* 2012) as described in Figure 3.

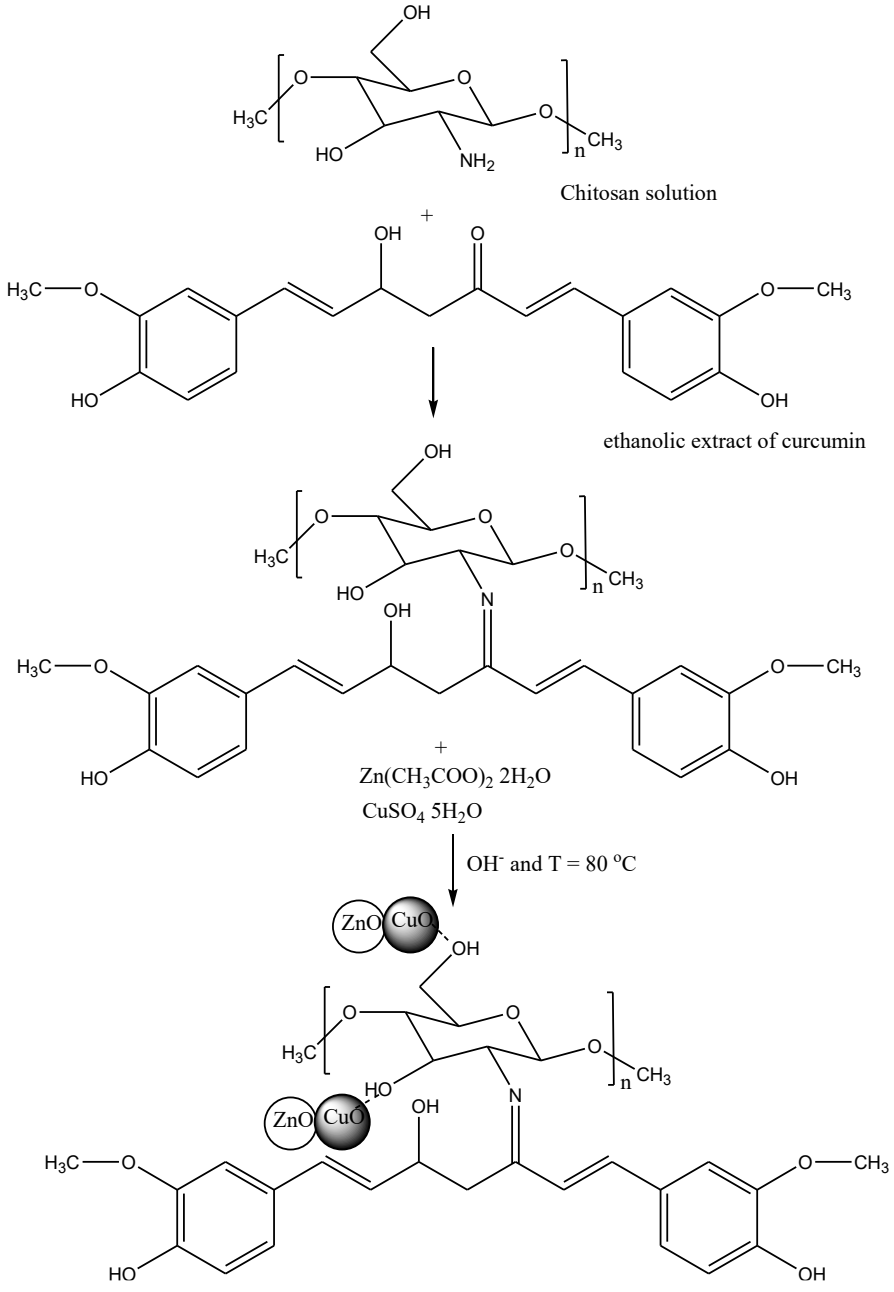


**Figure 3**. Reaction illustration of chitosan-curcumin-capped ZnO-CuO nanoparticles (Karthikeyan *et al.* 2020; Saranya *et al.* 2018; Kocak *et al.* 2012)

**XRD result**

XRD was used to study the structural analysis of the curcumin as functionalized ZnO-CuO nanoparticles, and the results are shown in Figure 4. In good agreement with the findings of Sathiyabama *et al.* (2020), the characteristic peaks of curcumin appeared at diffraction angles of 2θ at 16.58° with high intensity. Additionally, some peaks of lower intensity were observed at diffraction angles of 13.84°, 19.25°, and 28.15°. CuO nanoparticles were identified by distinctive peaks in the XRD pattern at a diffraction angle of 2θ at 35.80° (Kamble *et al.* 2016; Qasem *et al.* 2020; Varaprasad *et al*. 2020). The peaks observed in 2θ=32.40° and 59.3° confirmed the crystalline structure of zinc oxide nanoparticles (Cao *et al.* 2021; Kalpana *et al.* 2018)

The curcumin's physical structure analysis as functionalized chitosan-ZnO-CuO nanoparticles showed in Figure 5. The characteristics peaks of curcumin appeared at the diffraction angles of 2θ at 28.19° (low intensity). It was found that the CuO nanoparticles had main intensity peaks at 2θ =38.69° and 48.10° (Varaprasad *et al.* 2020; Qasem *et al.* 2020). The peak at 29.24° is $Cu_2O$ nanoparticles (Ranjan & Shukla 2025). XRD analysis of the ZnO nanoparticles shows diffraction peaks at 36.37°, 56.46°, 62.84° and 67.98° (Kalirajan & Palanisamy 2019). Chitosan peaks do not appear in this diffractogram, Ismail *et al.* (2022) reported the diffraction peaks became flatter and less noticeable when curcumin was added to the chitosan, suggesting that the crystallinity was lost. When these chemicals are introduced to chitosan, the crystallinity index drops and the polymer chains are less closely packed, which also causes a noticeable shift to a higher 2θ. This might be because active compounds and biopolymers interact more strongly via Van der Waals or H-bonds.

Equation 5 illustrates how the crystallite size of nanoparticles is determined using Debye Scherrer's formula.

$$D = (0.9\lambda / \beta.\cos\theta \quad ...(5)$$

In which D is the crystallite size in nm, λ is the wavelength of the incident radiation of Cu kα radiation (1.5406 Å), k is a constant (=0.89), θ and β are the diffraction angle and the full width at half maximum (FWHM) intensity, respectively. The crystallite size of curcumin as functionalized ZnO-CuO nanoparticles and curcumin as functionalized chitosan-ZnO-CuO nanoparticles was calculated by using the Debye–Scherrer equation were 1.88 and 12.58 nm respectively. The presence of other materials, such as ZnO-CuO nanoparticles, can also influence the crystallinity of chitosan-curcumin composites. These materials (ZnO-CuO nanoparticles) can interact with chitosan and curcumin, altering the overall crystallinity and morphology of the composite (Karthikeyan *et al.* 2020).

**SEM result**

Typical SEM images micrographs of curcumin as functionalized ZnO-CuO and curcumin as functionalized chitosan-ZnO-CuO nanoparticles are presented in Figure 5. The curcumin as functionalized chitosan-ZnO-CuO nanoparticles (Figure 5b) has a compressible surface structure. This is possible due to several things, such as the macropore structure is disturbed by the crystallization of curcumin on the porous structure of chitosan as reported by Wijayawardana *et al.* (2024). The morphology of ZnO-CuO nanoparticles are not very uniform, irregular-sized spherical structures

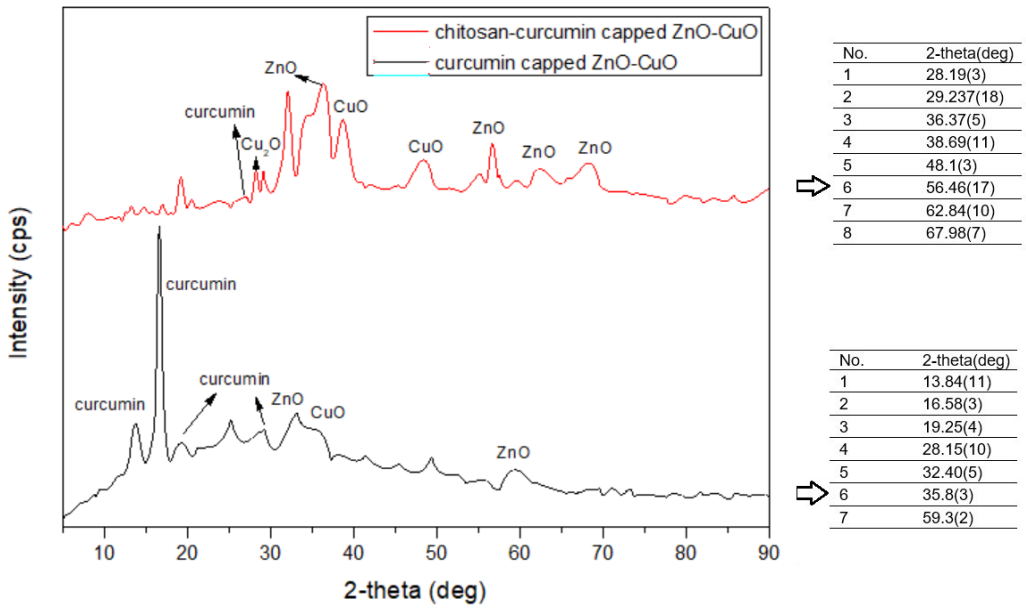


| No. | 2-theta(deg) |
|---|---|
| 1 | 28.19(3) |
| 2 | 29.237(18) |
| 3 | 36.37(5) |
| 4 | 38.69(11) |
| 5 | 48.1(3) |
| 6 | 56.46(17) |
| 7 | 62.84(10) |
| 8 | 67.98(7) |

| No. | 2-theta(deg) |
|---|---|
| 1 | 13.84(11) |
| 2 | 16.58(3) |
| 3 | 19.25(4) |
| 4 | 28.15(10) |
| 5 | 32.40(5) |
| 6 | 35.8(3) |
| 7 | 59.3(2) |

**Figure 4**. Curcumin-capped ZnO-CuO and chitosan-curcumin-capped ZnO-CuO nanoparticles' diffractogram

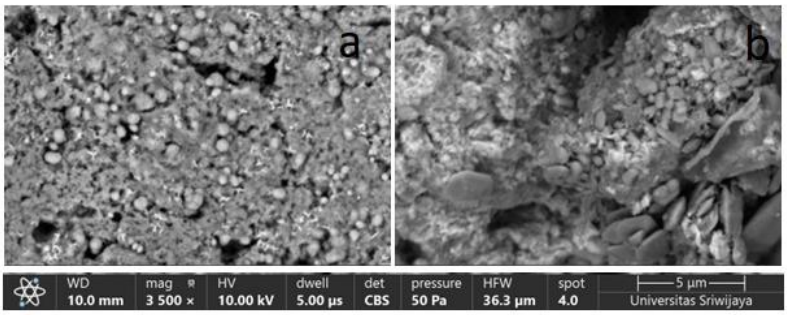


**Figure 5**. Structure morphology of curcumin-capped ZnO-CuO (a) and chitosan-curcumin-capped ZnO-CuO nanoparticles was analyzed using SEM at a magnification of x 3500 (b)

(Jeevarathinam & Asharani 2024) and most of the morphology exhibited nanosheet-like structure (Ma *et al.* 2016). Chitosan's amorphous nature can affect its interaction with other molecules (such as curcumin capped ZnO-CuO nanoparticles). The curcumin as functionalized ZnO-CuO nanoparticles also have a more compressible surface structure (Figure 5a). The combination of CuO and ZnO nanoparticles, indicating that this combination does not alter the overall structure of the curcumin as functionalized ZnO-CuO nanoparticles (Jeevarathinam & Asharani 2024).

**Antibacterial activity result**

Using different serial dilutions of the nanoparticles, as indicated in Table 1 and Figure 6, respectively the disc diffusion test was used to examine the antibacterial activity of the as-prepared curcumin-capped ZnO-CuO and chitosan-curcumin-capped ZnO-CuO nanoparticles.

*E. coli* was used to investigate the antibacterial activity and inhibitory zone of chloramphenicol, chitosan-curcumin-capped ZnO-CuO nanoparticles, and curcumin-capped ZnO-CuO nanoparticles (Figure 6 and Table 1). Every sample has antimicrobial properties. Interestingly, the ZnO-CuO nanoparticles capped with chitosan and curcumin had greater antibacterial activity than the ones covered with curcumin. The higher the concentration, the larger the inhibition zone formed.

Figure 7 shows an example of the antibacterial mechanism of ZnO-CuO nanoparticles coated with chitosan and curcumin. Explanation of Figure 7 includes: the antibacterial activity of nanoparticles is known to be governed by their surface composition and oxidative metal dissolution. Furthermore, the antibacterial mechanism of action of nanoparticles is also influenced by the presence of chitosan on them close to the surface. Chitosan adheres to the negative-charged cells of bacterial walls, triggering cell disruption and One mechanism that has been suggested is altering membrane permeability. Attachment to DNA follows, which prevents DNA replication and finally results in cell death (Mawazi *et al.* 2024).

Karthikeyan *et al.* (2020) examined how chitosan-curcumin-metal oxide nanoparticles interacted with bacterial cells, affecting the integrity of the cell membrane, membrane disarray, and macromolecule structural changes. Larger surface area, irregular outer surface ridges, and electrostatic attraction are examples of physical and chemical characteristics that significantly impact the antibacterial mechanism.

Bacterial cell membranes, which are created when two systems interact, are generally negatively charged, while $Zn^{2+}$ and $Cu^{2+}$ ions are positively charged. Along with an increase in oxygen vacancies and the transport ability of the reactant molecules (chitosan and curcumin), there is also a substantial stimulation of the release of $Zn^{2+}$ and $Cu^{2+}$ ions, which can cause oxidative stress within the bacterial cell and the creation of reactive oxygen species (ROS). ROS are oxygen-containing molecules composed of extremely unstable oxygen radicals, such as singlet oxygen ($O_2$), hydroxyl ($OH•$), superoxide ($O_2•$), and hydrogen peroxide ($H_2O_2$) (Takele *et al.* 2023; Perera *et al.* 2020).

Curcumin's low water solubility and low bioavailability severely limit its therapeutic utility, even though it and chitosan have well-established antibacterial qualities (Valencia *et al.* 2021). These results corroborate those of Karthikeyan *et al.* (2020), who also observed that curcumin and other agents that create nanomaterials have a synergistic impact against bacteria. Additionally, they show how curcumin, which is present in nanomaterials, can enhance the inhibition of bacterial growth, especially in Gram-negative bacteria.

Research indicates that the mechanism underlying curcumin's antibacterial activity varies depending on the strain being examined. Since curcumin's entry into bacteria is preferred in Gram-negative bacteria like *E. coli*, it can promote cell membrane permeabilization, which raises oxidative stress and causes DNA fragmentation and lipid peroxidation (Valencia *et al.* 2021). According to the justification provided, the nanoparticles' antimicrobial activity and curcumin release were both satisfactory. Chitosan's antibacterial properties may be explained by the way it’s positive amino groups interact electrostatically with the negatively charged components on the

**Table 1**. Inhibition zones produced by curcumin-capped ZnO-CuO, chitosan-curcumin-capped ZnO-CuO nanoparticles, chloramphenicol and DMSO respectively

| Test compound | Concentration (%) | Zone of inhibition (mm) | | | |
|---|---|---|---|---|---|
| | | 1 | 2 | 3 | Average |
| Curcumin-capped ZnO-CuO | 1.5 | 7.80 | 8.56 | 9.74 | 8.70 ± 0.97 |
| nanoparticles | 2 | 8.84 | 9.21 | 10.52 | 9.52 ± 0.88 |
| chitosan-curcumin-capped ZnO-CuO | 1.5 | 9.22 | 9.87 | 11.10 | 10.06 ± 0.95 |
| nanoparticles | 2 | 9.88 | 15.45 | 18.50 | 14.61 ± 4.37 |
| chloramphenicol | 0.01 | 12.15 | 11.54 | 10.49 | 11.39 ± 0.83 |
| DMSO | - | 0 | 0 | 0 | 0 |

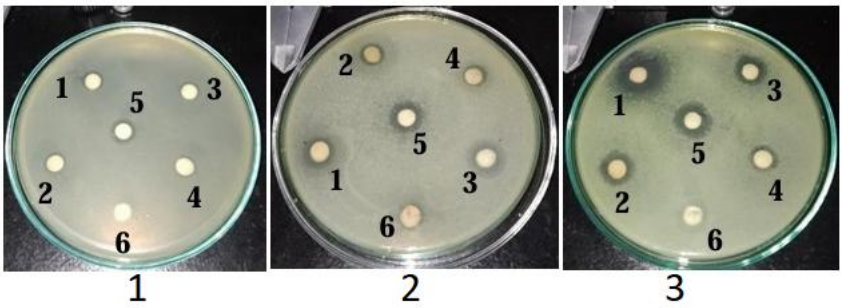


**Figure 6.** Curcumin-capped ZnO-CuO nanoparticles (1,2), chitosan-curcumin-capped ZnO-CuO nanoparticles (3,4), chloramphenicol (5), and DMSO (6) all exhibit antibacterial properties

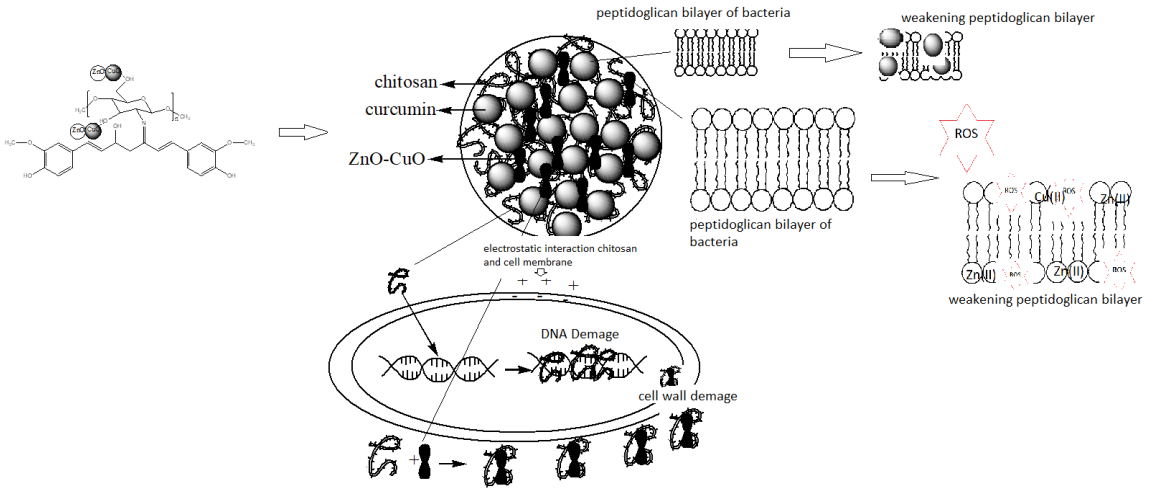


**Figure 7**. An example of how chitosan-curcumin-capped ZnO-CuO nanoparticles work as antibacterial agents (Perera *et al.* 2020; Dhlamini *et al.* 2024)

bacterial cell surface. As a result, chitosan may cause intracellular components to leak out (Li & Zhuang 2020; Meng *et al.* 2020; Dhlamini *et al.* 2024).

## CONCLUSION

It is possible to biofabricate the chitosan-curcumin-capped ZnO-CuO and curcumin-capped ZnO-CuO nanoparticles. Both FTIR spectra show that the groups of Zn-O and Cu-O are detected in the range of 500-700 $cm^{-1}$. The crystalline form was shown by the XRD pattern of the curcumin-capped ZnO-CuO and chitosan-curcumin-capped ZnO-CuO nanoparticles. The surface appearance of ZnO-CuO covered with chitosan and curcumin and curcumin-capped ZnO-CuO nanoparticles is a compressible surface structure. Chitosan-curcumin-capped ZnO-CuO nanoparticles have more antibacterial activity against *E. coli* bacteria than do curcumin-capped ZnO-CuO nanoparticles. Chitosan-curcumin-capped ZnO-CuO nanoparticles showed the most promising activity against tested bacterial strains. Chitosan enhances antibacterial activity through various mechanisms, primarily by interacting with bacterial cell membranes and disrupting their function. Our findings highlight the applicability of using curcumin-capped ZnO-CuO and chitosan-curcumin-

capped ZnO-CuO nanoparticles considering the potential impact of the capping process on actibacterial activity. Future work on this study should focus on optimizing synthesis methods for enhanced properties, investigate their potential in various fields like food packaging, exploring their applications in drug delivery and wound healing, and investigating their long-term stability and biocompatibility.

**ACKNOWLEDGMENT**

We are grateful to STIFI Bhakti Pertiwi for providing money for this study.

**REFERENCES**

Abbas, H.M., Al Marjani, M.F. & Gdoura, R. (2024). Evaluation of the antibacterial activity of CuO and ZnO nanoparticles against uropathogenic Escherichia coli. *Journal of Taibah University for Science*. **18(1)**: 1-12.

Adeyemi, J.O., Onwudiwe, D.C. & Oyedeji, A. O. (2022). Biogenic synthesis of CuO, ZnO, and CuO–ZnO nanoparticles using leaf extracts of Dovyalis caffra and their biological properties. *Molecules*. **27(10)**: 1-15.

Aigbe, U.O. & Osibote, O.A. (2024). Green synthesis of metal oxide nanoparticles, and their various applications. *Journal of Hazardous Materials Advances*. **13**: 1-49.

Alallam, B., Doolaanea, A.A., Alfatama, M. & Lim, V. (2023). Phytofabrication and characterisation of zinc oxide nanoparticles using pure curcumin. *Pharmaceuticals*. **16(2)**: 1-23.

Ali, S.A., Ali, E.S., Hamdy, G., Badawy, M.S.E., Ismail, A.R., El-Sabbagh, I.A., El-Fass, M.M. & Elsawy, M.A. (2024). Enhancing physical characteristics and antibacterial efficacy of chitosan through investigation of microwave-assisted chemically formulated chitosan-coated ZnO and chitosan/ZnO physical composite. *Scientific Reports*. **14(1)**: 9348.

Al-Rajhi, A.M., Abdelghany, T.M., Almuhayawi, M. S., Alruhaili, M.H., Al Jaouni, S.K. & Selim, S. (2024). The green approach of chitosan/Fe2O3/ZnO-nanocomposite synthesis with an evaluation of its biological activities. *Applied Biological Chemistry*. **67(1)**: 1-13.

Alzahrani, E. (2018). Chitosan membrane embedded with ZnO/CuO nanocomposites for the photodegradation of fast green dye under artificial and solar irradiation. *Analytical Chemistry Insights*. **13**: 1-13.

Arab, C., El Kurdi, R. & Patra, D. (2021). Chitosan coated zinc curcumin oxide nanoparticles for the determination of ascorbic acid. *Journal of Molecular Liquids*. **328**: 115504.

Azkia, A., Baihaqi, A.I., Prabowo, H.A., Handayani, S. & Agustiany, T. (2020). A preliminary study on modified chitosan-curcuminoids as material active food packaging with antioxidant and antibacterial activities. *In IOP Conference Series: Materials Science and Engineering*. **902(1)**: 012040

Bekru, A.G., Tufa, L.T., Zelekew, O.A., Goddati, M. Lee, J. & Sabir, F.K. (2022). Green synthesis of a CuO–ZnO nanocomposite for efficient photodegradation of methylene blue and reduction of 4-nitrophenol. *ACS Omega*. **7(35)**: 30908-30919.

Bordiwala, R.V. (2023). Green synthesis and applications of metal nanoparticles.-A review article. *Results in Chemistry*. **5**: 1-4.

Cao, Y., Dhahad, H.A., El-Shorbagy, M.A., Alijani, H.Q., Zakeri, M., Heydari, A. Bahonar, E., Slouf, M., Khatami, M., Naderifar, M., Iravani, S., Khatami, S. & Dehkordi, F.F. (2021). Green synthesis of bimetallic ZnO–CuO nanoparticles and their cytotoxicity properties. *Scientific Reports*. **11(1)**: 23479.

da Rocha, L.V.M., Merat, L.C., de Menezes, L.R., Finotelli, P.V., da Silva, P.S.R.C. & Tavares, M.I.B. (2020). Extract of curcuminoids loaded on polycaprolactone and pluronic nanoparticles: chemical and structural properties. *Applied Nanoscience*. **10(4)**: 1141-1156.

Dadi, R., Azouani, R., Traore, M., Mielcarek, C. & Kanaev, A. (2019). Antibacterial activity of ZnO and CuO nanoparticles against gram positive and gram negative strains. *Materials Science and Engineering: C*. **104**: 1-9.

Deepika, D., Prasad, M., Salar, A. & Salar, R. K. (2022). In vitro anticancer activity of curcumin loaded chitosan nanoparticles (CLCNPs) against Vero cells. *Pharmacological Research-Modern Chinese Medicine*. **3**: 1-9.

Dhage, S.B. Sah, P.M., Lakkakula, J., Raut, R.W., Malghe, Y.S., Roy, A., Verma, D. & Kaur, K. (2024). ZnO-CuO nanocomposite synthesized by co-precipitation: Characterization and antibacterial properties. *Biointerface Research in Applied Chemistry*. **14(3)**: 1-10.

Dhlamini, K.S., Selepe, C.T., Ramalapa, B., Tshweu, L. & Ray, S.S. (2024). Reimagining chitosan-based antimicrobial biomaterials to mitigate antibiotic resistance and alleviate antibiotic overuse: *A Review. Macromolecular Materials and Engineering*. **309(9)**: 1-31.

El-Kattan, N., Emam, A.N., Mansour, A.S., Ibrahim, M.A., Abd El-Razik, A.B., Allam, K.A., Riad, N.Y. & Ibrahim, S.A. (2022). Curcumin assisted green synthesis of silver and zinc oxide nanostructures and their antibacterial activity against some clinical pathogenic multi-drug resistant bacteria. *RSC Advances*. **12(28)**: 18022-18038.

El-Naggar, N.E.A., Shiha, A.M., Mahrous, H. & Mohammed, A.A. (2022). Green synthesis of chitosan nanoparticles, optimization, characterization and antibacterial efficacy against multi drug resistant biofilm-forming

Acinetobacter baumannii. *Scientific Reports*. **12(1)**: 19869.

Enumo Jr, A., Argenta, D.F., Bazzo, G.C., Caon, T., Stulzer, H.K. & Parize, A.L. (2020). Development of curcumin-loaded chitosan/pluronic membranes for wound healing applications. *International Journal of Biological Macromolecules*. **163**: 167-179.

Etemadi, S., Barhaghi, M.S., Leylabadlo, H.E., Memar, M.Y., Mohammadi, A.B. & Ghotaslou, R. (2021). The synergistic effect of turmeric aqueous extract and chitosan against multidrug-resistant bacteria. *New Microbes and New Infections*. **41**: 1-8.

Fatoni, A., Hasanah, M., Sirumapea, L., Putri, A.D., Sari, K., Khairani, R.D. & Hidayati, N. (2023a). Synthesis, characterization of polyvinyl alcohol-chitosan-ZnO/CuO nanoparticles film and its biological evaluation as an antibacterial agent of *Staphylococcus aureus*. *Al Kimiya: Jurnal Ilmu Kimia dan Terapan*. **10(1)**: 1-12.

Fatoni, A., Rendowati, A., Sirumapea, L., Miranti, L., Masitoh, S. & Hidayati, N. (2023b). Synthesis, characterization of Chitosan-ZnO/CuO nanoparticles film, and its effect as an antibacterial agent of *Escherichia coli*. *Science and Technology Indonesia*. **8(3)**: 373-381.

Gamboa-Solana, C.D.C., Chuc-Gamboa, M.G., Aguilar-Pérez, F.J., Cauich-Rodríguez, J.V., Vargas-Coronado, R.F., Aguilar-Pérez, D.A., Cauich-Rodríguez, J.V., Vargas-Coronado, R.F., Aguilar-Pérez, D.A., Herrera-Atoche, J.R. & Pacheco, N. (2021). Zinc oxide and copper chitosan composite films with antimicrobial activity. *Polymers*. **13(22)**: 1-17.

Govindasamy, G.A., Mydin, R.B.S., Sreekantan, S.,& Harun, N.H. (2021). Compositions and antimicrobial properties of binary ZnO–CuO nanocomposites encapsulated calcium and carbon from Calotropis gigantea targeted for skin pathogens. Scientific Reports. **11(1)**: 1-14.

Ismail, K.A., El Askary, A., Farea, M.O., Awwad, N. S., Ibrahium, H.A., Moustapha, M.E. & Menazea, A.A. (2022). Perspectives on composite films of chitosan-based natural products (Ginger, Curcumin, and Cinnamon) as biomaterials for wound dressing. *Arabian Journal of Chemistry*. **15(4)**: 103716.

Isnaeni, I., Hendradi, E. & Zettira, N. Z. (2020). *Hibiscus sabdariffa* l sulu ekstrelerini içeren HPMC 6000 jel formülasyonunun S*taphylococcus aureus* ATCC 25923 büyümesi üzerine inhibitör etkisi. *Turkish Journal of Pharmaceutical Sciences*. **17(2)**: 190-196.

Jahromi, M.A.M., Al Musawi, S., Pirestani, M., Fasihi, R.M., Ahmadi, K., Rajayi, H., Hassan, Z.M., Kamali, M. & Mirnejad, R. (2014). Curcumin-loaded chitosan tripolyphosphate nanoparticles as a safe, natural and effective antibiotic inhibits the infection of *Staphylococcus aureus* and *Pseudomonas aeruginosa* in vivo. *Iranian Journal of Biotechnology*. **12(3)**: 1-8.

Jeevarathinam, M. & Asharani, I.V. (2024). Synthesis of CuO, ZnO nanoparticles, and CuO-ZnO nanocomposite for enhanced photocatalytic degradation of Rhodamine B: a comparative study. *Scientific Reports*. **14(1)**: 1-37.

Kabiriyel, J., Jeyanthi, R., Jayakumar, K., Amalraj, A., Arjun, P., Shanmugarathinam, A., Vignesh, G. & Mohan, C.R. (2023). Green synthesis of carboxy methyl chitosan based curcumin nanoparticles and its biological activity: Influence of size and conductivity. *Carbohydrate Polymer Technologies and Applications*. **5**: 1-7.

Kalia, A., Kaur, M., Shami, A., Jawandha, S.K., Alghuthaymi, M.A., Thakur, A. & Abd-Elsalam, K.A. (2021). Nettle-leaf extract derived ZnO/CuO nanoparticle-biopolymer-based antioxidant and antimicrobial nanocomposite packaging films and their impact on extending the post-harvest shelf life of guava fruit. *Biomolecules*. **11(2)**: 1-24.

Kalirajan, C. & Palanisamy, T. (2019). A ZnO–curcumin nanocomposite embedded hybrid collagen scaffold for effective scarless skin regeneration in acute burn injury. *Journal of Materials Chemistry B*. **7(38)**: 5873-5886.

Kalpana, V.N., Kataru, B.A.S., Sravani, N., Vigneshwari, T., Panneerselvam, A. & Rajeswari, V.D. (2018). Biosynthesis of zinc oxide nanoparticles using culture filtrates of *Aspergillus niger*: Antimicrobial textiles and dye degradation studies. *OpenNano*. **3**: 48-55.

Kamble, S., Utage, B., Mogle, P., Kamble, R., Hese, S., Dawane, B. & Gacche, R. (2016). Evaluation of curcumin capped copper nanoparticles as possible inhibitors of human breast cancer cells and angiogenesis: a comparative study with native curcumin. *American Association of Pharmaceutical Scientists*. **17(5)**: 1030-1041.

Karthikeyan, C., Varaprasad, K., Akbari-Fakhrabadi, A., Hameed, A.S.H. & Sadiku, R. (2020). Biomolecule chitosan, curcumin and ZnO-based antibacterial nanomaterial, via a one-pot process. *Carbohydrate Polymers*. **249**: 1-12.

Khalil, M.M., Ismail, E.H., El-Baghdady, K.Z. & Mohamed, D. (2014). Green synthesis of silver nanoparticles using olive leaf extract and its antibacterial activity. *Arabian Journal of Chemistry*. **7(6)**: 1131-1139.

Khezri, A., Karimi, A., Yazdian, F., Jokar, M., Mofradnia, S.R., Rashedi, H. & Tavakoli, Z. (2018). Molecular dynamic of curcumin/chitosan interaction using a computational molecular approach: Emphasis on biofilm reduction. *International Journal of Biological Macromolecules*. **114**: 972-978.

Kocak, N., Sahin, M., Kücükkolbasi, S. & Erdogan, Z. O. (2012). Synthesis and characterization of novel nano-chitosan Schiff base and use of lead (II) sensor. International Journal of Biological Macromolecules. **51(5)**: 1159-1166.

Li, J. & Zhuang, S. (2020). Antibacterial activity of chitosan and its derivatives and their interaction mechanism with bacteria: Current state and perspectives. *European Polymer Journal*. **138**: 1-12.

Liu, Y., Cai, Y., Jiang, X., Wu, J. & Le, X. (2016). Molecular interactions, characterization and antimicrobial activity of curcumin–chitosan blend films. *Food Hydrocolloids*. **52**: 564-572.

Ma, X., Zhang, B., Cong, Q., He, X., Gao, M. & Li, G. (2016). Organic/inorganic nanocomposites of ZnO/CuO/chitosan with improved properties. *Materials Chemistry and Physics*. **178**: 88-97.

Madeo, L. F., Schirmer, C., Cirillo, G., Froeschke, S., Hantusch, M., Curcio, M., Nicoletta, F.P., Büchner, B., Mertig, M. & Hampel, S. (2023). Facile one-pot hydrothermal synthesis of a zinc oxide/curcumin nanocomposite with enhanced toxic activity against breast cancer cells. *RSC Advances*. **13(39)**: 27180-27189.

Madian, N.G., El-Ashmanty, B.A. & Abdel-Rahim, H.K. (2023). Improvement of chitosan films properties by blending with cellulose, honey and curcumin. *Polymers.* **15(12)**: 1-22.

Malik, S., Muhammad, K. & Waheed, Y. (2023). Nanotechnology: a revolution in modern industry. *Molecules*. **28(2)**: 1-26.

Mawazi, S.M., Kumar, M., Ahmad, N., Ge, Y. & Mahmood, S. (2024). Recent applications of chitosan and its derivatives in antibacterial, anticancer, wound healing, and tissue engineering fields. *Polymers*. **16(10)**: 1-134.

Meng, D., Garba, B., Ren, Y., Yao, M., Xia, X., Li, M. & Wang, Y. (2020). Antifungal activity of chitosan against Aspergillus ochraceus and its possible mechanisms of action. International Journal of Biological Macromolecules. **158**: 1063-1070.

Mohammadi, F.M. & Ghasemi, N. (2018). Influence of temperature and concentration on biosynthesis and characterization of zinc oxide nanoparticles using cherry extract. *Journal of Nanostructure in Chemistry*. **8(1)**: 93-102.

Mosallanezhad, P., Nazockdast, H., Ahmadi, Z. & Rostami, A. (2022). Fabrication and characterization of polycaprolactone/chitosan nanofibers containing antibacterial agents of curcumin and ZnO nanoparticles for use as wound dressing. Frontiers in Bioengineering and Biotechnology. **10**: 01-14.

Moussawi, R.N. & Patra, D. (2016). Modification of nanostructured ZnO surfaces with curcumin: fluorescence-based sensing for arsenic and improving arsenic removal by ZnO. *RSC Advances*. **6(21)**: 17256-17268.

Nepal, P., Parajuli, S., Awasthi, G.P., Sharma, K.P., Oli, H.B., Shrestha, R.L. & Bhattarai, D.P. (2024). Eco-Friendly Synthesis of CuO@ ZnO Nanocomposites using *Artemisia vulgaris* leaf extract and study of its photocatalytic activity for methylene blue. *Journal of Nanotechnology*. **2024(1)**: 1-15.

Nguyen, N.T., Nguyen, N.T. & Nguyen, V.A. (2020). In situ synthesis and characterization of ZnO/chitosan nanocomposite as an adsorbent for removal of Congo red from aqueous solution. *Advances in Polymer Technology*. **2020(1)**: 1-8.

Orshiso, T.A., Zereffa, E.A., Murthy, H.A., Demissie, T.B., Pardeshi, O., Avhad, L.S. & Ghotekar, S. (2023). Biosynthesis of Artemisia abyssinica leaf extract-mediated bimetallic ZnO–CuO nanoparticles: antioxidant, anticancer, and molecular docking studies. *ACS Omega*. **8(44)**: 41039-41053.

Patra, D. & El Kurdi, R. (2021). Curcumin as a novel reducing and stabilizing agent for the green synthesis of metallic nanoparticles. *Green Chemistry Letters and Reviews*. **14(3)**: 474-487.

Perera, W.P.T.D., Dissanayake, R.K., Ranatunga, U. I., Hettiarachchi, N.M., Perera, K.D.C., Unagolla, J.M., De Silva, R.T. & Pahalagedara, L.R. (2020). Curcumin loaded zinc oxide nanoparticles for activity-enhanced antibacterial and anticancer applications. *RSC Advances*. **10(51)**: 30785-30795.

Qasem, M., El Kurdi, R. & Patra, D. (2020). Green synthesis of curcumin conjugated CuO nanoparticles for catalytic reduction of methylene blue. *ChemistrySelect*. **5(5)**: 1694-1704.

Rachtanapun, P., Klunklin, W., Jantrawut, P., Jantanasakulwong, K., Phimolsiripol, Y., Seesuriyachan, P., Leksawasdi, N., Chaiyaso, T., Ruksiriwanich, W., Phongthai, S., Sommano, S.R., Punyodom, W., Reungsang, A. & Ngo, T.M.P. (2021). Characterization of chitosan film incorporated with curcumin extract. *Polymers*. **13(6)**: 963.

Ramalingam, B., Khan, M.M.R., Mondal, B., Mandal, A.B. & Das, S.K. (2015). Facile synthesis of silver nanoparticles decorated magnetic-chitosan microsphere for efficient removal of dyes and microbial contaminants. ACS *Sustainable Chemistry & Engineering*. **3(9)**: 2291-2302.

Ranjan, R. & Shukla, M. (2025). Curcumin-mediated synthesis of cuprous oxide nanoparticles and its photocatalytic application. *Next Materials*. **6**: 1-7.

Ren, E., Zhang, C., Li, D., Pang, X. & Liu, G. (2020). Leveraging metal oxide nanoparticles for bacteria tracing and eradicating. *View*. **1(3)**: 1-15.

Saif, A., Omer, M. O., Sattar, A., Tipu, Y., Alharbi, H. M., Saher, U. & Awan, T. (2024). Comprehensive analysis of curcumin zinc oxide nanoparticles, synthesis, characterization, and cytogenotoxic profiling. *ACS Omega*. **9(26)**: 28186-28193.

Sanmugam, A., Sellappan, L.K., Sridharan, A., Manoharan, S., Sairam, A.B., Almansour, A.I., Veerasundaram, S., Kim, H. & Vikraman, D. (2024). Chitosan-integrated curcumin–graphene oxide/copper oxide hybrid nanocomposites for antibacterial and cytotoxicity applications. *Antibiotics*. **13(7)**: 1-15.

Saranya, T. S., Rajan, V. K., Biswas, R., Jayakumar, R. & Sathianarayanan, S. (2018). Synthesis, characterisation and biomedical applications of curcumin conjugated chitosan microspheres. International Journal of Biological Macromolecules. **110**: 227-233.

Sathiyabama, M., Indhumathi, M. & Amutha, T. (2020). Preparation and characterization of curcumin functionalized copper nanoparticles and their application enhances disease resistance in chickpea against wilt pathogen. *Biocatalysis and Agricultural Biotechnology*. **29**: 1-7.

Soumya, K.R., Snigdha, S., Sugathan, S., Mathew, J. & Radhakrishnan, E.K. (2017). Zinc oxide–curcumin nanocomposite loaded collagen membrane as an effective material against methicillin-resistant coagulase-negative Staphylococci. *3 Biotech*. **7(4)**: 1-10.

Szczyglewska, P., Feliczak-Guzik, A. & Nowak, I. (2023). Nanotechnology–general aspects: A chemical reduction approach to the synthesis of nanoparticles. *Molecules*. **28(13)**: 1-38.

Takele, E., Feyisa Bogale, R., Shumi, G. & Kenasa, G. (2023). Green synthesis, characterization, and antibacterial activity of CuO/ZnO nanocomposite using *Zingiber officinale* rhizome extract. *Journal of Chemistry*. **2023(1)**: 1-15.

Valencia, M.S., da Silva Júnior, M.F., Xavier-Júnior, F.H., de Oliveira Veras, B., de Albuquerque, P.B.S., de Oliveira Borba, E.F., da Silva, T.G., Lansky Xavier, V., de Souza, M. P. & das Graças Carneiro-da-Cunha, M. (2021). Characterization of curcumin-loaded lecithin-chitosan bioactive nanoparticles. *Carbohydrate Polymer Technologies and Applications*. **2**: 1-9.

Varaprasad, K., López, M., Núñez, D., Jayaramudu, T., Sadiku, E. R., Karthikeyan, C. & Oyarzúnc, P. (2020). Antibiotic copper oxide-curcumin nanomaterials for antibacterial applications. *Journal of Molecular Liquids*. **300**: 1-8.

Venkatas, J., Daniels, A. & Singh, M. (2022). The potential of curcumin-capped nanoparticle synthesis in cancer therapy: a green synthesis approach. *Nanomaterials*. **12(18)**: 1-23.

Widiarti, N., Sae, J.K. & Wahyuni, S. (2017). Synthesis CuO-ZnO nanocomposite and its application as an antibacterial agent. *In IOP Conference Series: Materials Science and Engineering*. **172(1)**: 012036.

Wijayawardana, S., Thambiliyagodage, C. & Jayanetti, M. (2024). Kinetic study of in vitro release of curcumin from chitosan biopolymer and the evaluation of biological efficacy. *Arabian Journal of Chemistry*. **17(9)**: 1-17.

Yazdani, Z., Mehrgan, M.S., Khayatzadeh, J., Shekarabi, S.P.H., & Tabrizi, M.H. (2023). Dietary green-synthesized curcumin-mediated zinc oxide nanoparticles promote growth performance, haemato-biochemical profile, antioxidant status, immunity, and carcass quality in Nile tilapia (*Oreochromis niloticus*). *Aquaculture Reports*. **32**: 1-11.

Yousefinia, A., Khodadadi, M. & Mortazavi-Derazkola, S. (2023). An efficient biosynthesis of novel ZnO/CuO nanocomposites using berberis vulgaris extract (ZnO/CuO@ BVENCs) for enhanced photocatalytic degradation of pollution, antibacterial and antifungal activity. *Environmental Technology & Innovation*. **32**: 1-14.

Zulkifli, M.D., Yusefi, M., Shameli, K. & Teow, S. Y. (2022). Curcumin extract loaded with chitosan nanocomposite for cancer treatment. *Journal of Research in Nanoscience and Nanotechnology*. **6(1)**: 1-13.